Science Forum (Journal of Pure and Applied Sciences)

Journal Homepage: https://atbu.edu.ng/science-forum/

Thermal Evolution of the Oceanic Lithosphere Along the Western Coast of Africa: A Comparative Analysis of Cooling Models.

Usman Yahaya Yaro

Department of Applied Geology, Faculty of Science, Abubakar Tafawa Balewa University, P.M.B. 0248, Bauchi, Nigeria.

ABSTRACT

This study investigates the evolution of the oceanic lithosphere along the Western Coast of Africa by evaluating two prominent theoretical models: the half-space cooling model and the plate model. Through a detailed analysis of geothermal behavior, the research explores the variations in predicted temperature structures and their implications for lithospheric dynamics. The findings reveal distinct thermal patterns, with elevated temperatures observed beneath the ocean ridges, consistent with active magmatic processes. As the lithosphere moves away from the ridge axis, a clear cooling trend is identified, aligning with the theoretical predictions of both models. However, discrepancies arise in the rate and extent of cooling, particularly at greater distances from the ridge, suggesting limitations in the assumptions of the half-space cooling model. The plate model, incorporating a fixed basal temperature, provides a more robust framework for explaining the observed thermal gradients. These insights enhance our understanding of lithospheric evolution and have significant implications for plate tectonics, mantle dynamics, and geothermal resource potential in the region. The study underscores the importance of integrating observational data with theoretical models to refine our knowledge of Earth's thermal and mechanical processes.

ARTICLE INFO

Received 12 August 2024
Received in Revised Form 21 August 2024
Accepted 2nd September 2024
Published 1st November 2024
Available online 1st November 2024

KEYWORDS

Thermal Evolution,
Oceanic Lithosphere,
Western Coast of Africa,
Analysis of Cooling Models.

Corresponding Author: Usman Yahaya Yaro ✉ usmangeophysics@gmail.com ✉ Department of Applied Geology, Faculty of Science, Abubakar Tafawa Balewa University, P.M.B. 0248, Bauchi, Nigeria.

1. Introduction

The primary aim of this study is to investigate the shallow thermal structure of the oceanic lithosphere for the West African margin, with focus on areas that have basins and oil and gas prospectivity. The lithosphere is often defined thermally (Goutorbe, 2010; Mckenzie, 1967; Sleep, 2005; Turcotte and Oxburgh, 1967) because of the strong dependence of rock strength on temperature. The lower boundary of the lithosphere is described to be an isotherm in which materials lying above it are cool and rigid, and those below it is hot to deform easily.

The thermal structure and evolution of the oceanic lithosphere is an important component of the Earth's interior, since temperature controls the physical properties of the lithosphere. There are two fundamental models for calculating the temperature structure of the oceanic lithosphere; the half space cooling model (derived by Turcotte and Oxburgh, 1967) and the plate model (derived by Mckenzie, 1967). Both models assume that the two lithospheric plates moves apart and that heat transport is predominantly by conduction (besides near the ridge crest). Although, the two models have the same prediction for young plates, but they vary significantly above 50 Ma for heat flow predictions and 80 Ma for depth of the ocean floor predictions.

Measurement of surface heat flow is very expensive and difficult to undertake since it requires the drilling of a borehole and also involves measuring a gradient at or near the contact between two different substances; water and sediments for oceans and rocks and air for continents. As a result, attention has been directed towards developing theoretical models for predicting the evolution of oceanic lithosphere.

Heat flow data are very sparse near the ocean ridges with high and low values (fig. 1). A plot of heat flow versus age for the western coast of Africa shows a continuous decrease in heat flow from the younger to the older crust (fig. 2). A linear regression and 4^{th} order polynomial were used to fit the data because of the scatter in the data. For better fit, the data for younger (<50Ma) crust shows a corresponding decrease in heat flow away from the ridge. Older age (>51 -180Ma) crust heat flow values are linear and almost close to equilibrium.

The continuous decrease in heat flow away from the ridge crest and its constant linear pattern for older age crust is in line with the model in which hot materials are intruded near the ridge crest and as the new crust move away from the ridge heat is lost by conduction. In addition, the flattening of the heat flow data for older age shows that the plate model might provide the best fit to the data.

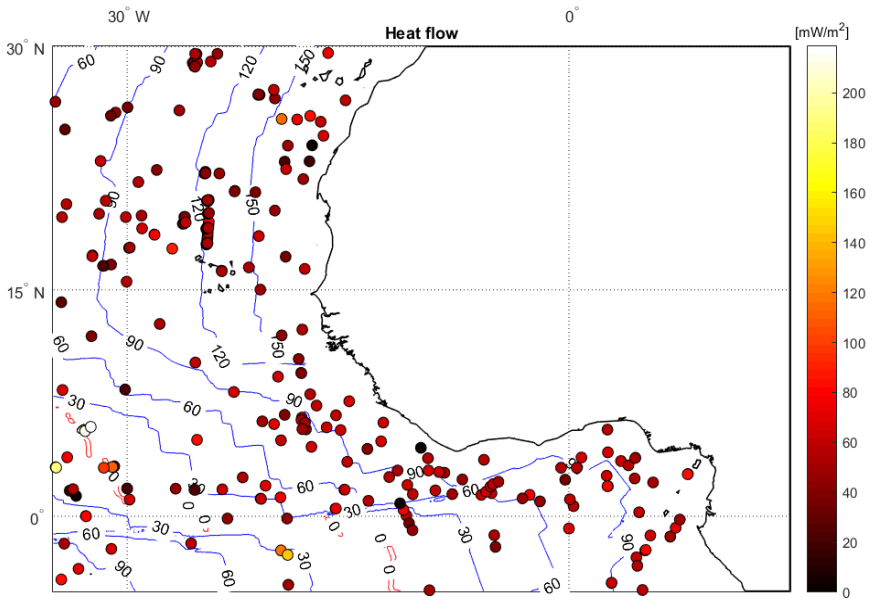

Figure 1: Heat flow map for the western coast of Africa. Blue lines indicate ocean age, red lines indicate the ocean ridge and small coloured circles indicate heat flow data point. Heat flow data was deduced from the global heat flow database of the International Heat flow Commission (2006) and seafloor age was deduced from Muller et al., (2008).

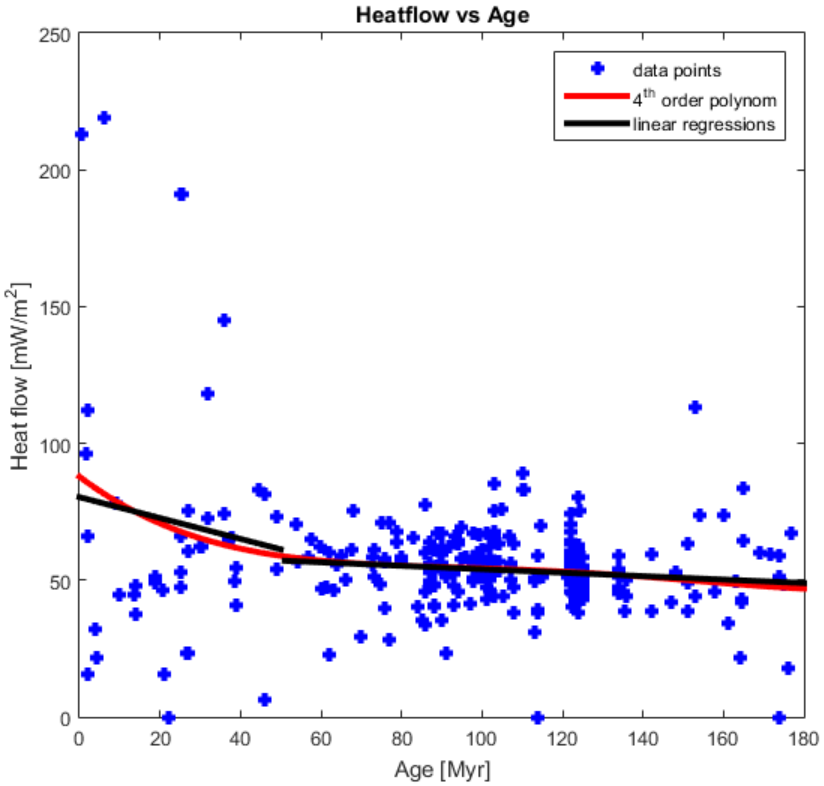

Figure 2: Seafloor age-heat flow relations for the western margin of Africa (heat flow data adopted from the International Heat flow Commission, 2006).

2 Review of cooling models

2.1 Thermal models of the lithosphere

Conduction is the dominant mode of heat transfer in the lithosphere except in regions affected by magmatic and hydrothermal processes. The temperature distribution in the lithosphere can be estimated by solving the general equation of heat conduction. Similarly, the thermal condition of the continental lithosphere is different from that of oceanic lithosphere. In the continental lithosphere there is often no variation of temperature with age, at least in shields and cratons, and the radiogenic heat production is high. However, radiogenic heat is negligible in the oceanic lithosphere and there is dependence on the variation of temperature with time.

Time after time different theoretical models have been developed to predict the thermal structure of ocean lithosphere. The two classes of lithospheric cooling models that give the best fit to heat flow data and ocean floor depth are discussed here.

2.1.1 Half – space cooling model

Temperature in the ocean lithosphere can be described by a half – space cooling model, in which hot material at the ridge cools as the oceanic plate drifts away from the ridge axis (Stein et al., 2003). This gives rise to changes in heat flow and seafloor bathymetry owing to thickening of the oceanic lithosphere from the ridge axis. The variation of temperature with age and depth can be derived from Turcotte and Oxburgh, (1967). The temperature (T (z, t)) as a function of depth and time of the conductive layer is expressed thus;

$$T(z, t) = Ts + (Tm - Ts)\ erf\left(\frac{z}{2\sqrt{kt}}\right) \ldots (2.1)$$

Where z, is depth in kilometer, and t, is the apparent thermal age, and Tm, is the initial mantle temperature = 1300^0C, Ts, is the surface temperature = 0^0C and erf, is the error function. Figure 3 shows the variation of the erf between erf (0) = 0 and erf (3) ≈ 1. The thermal diffusivity (k) is measured in m^2s^{-2}. Since the oceanic lithosphere is fast spreading from the ridge than heat is conducted horizontally, only vertical heat conduction is considered (Stein et al., 2003). Thus, the temperature is inversely proportional to the square root of lithospheric age.

Analysis of the half space cooling model enable the prediction of cooling of the oceanic lithosphere as it moves away from the oceanic ridges. Isotherms calculated from this model are shown in Figure 4, which shows the variation of temperature with age and depth. The plot show continues cooling of oceanic isotherms (for ages 0 – 180 Ma) as it moves away from the ridge axis. The depth to these isotherms increases with lithospheric age. However, the half space model proposed by Turcotte and Oxburgh (1967) assume there is no external heat source at the base of the plate, and so only the heat produced at the spreading ridge is taken into consideration.

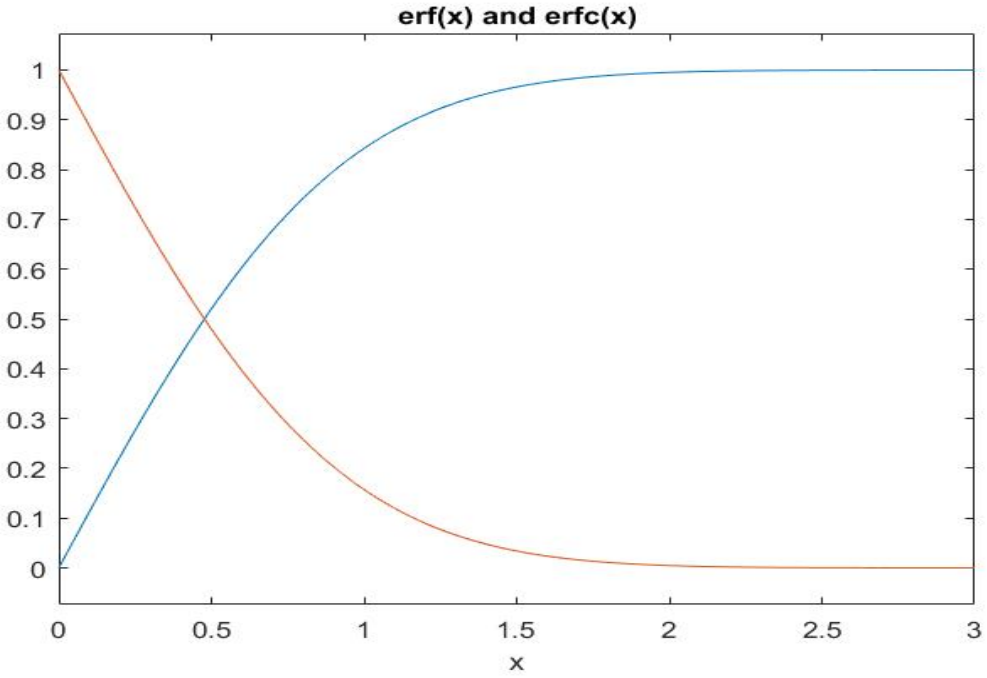

Figure 3: Plot of error function, which controls the cooling solution.

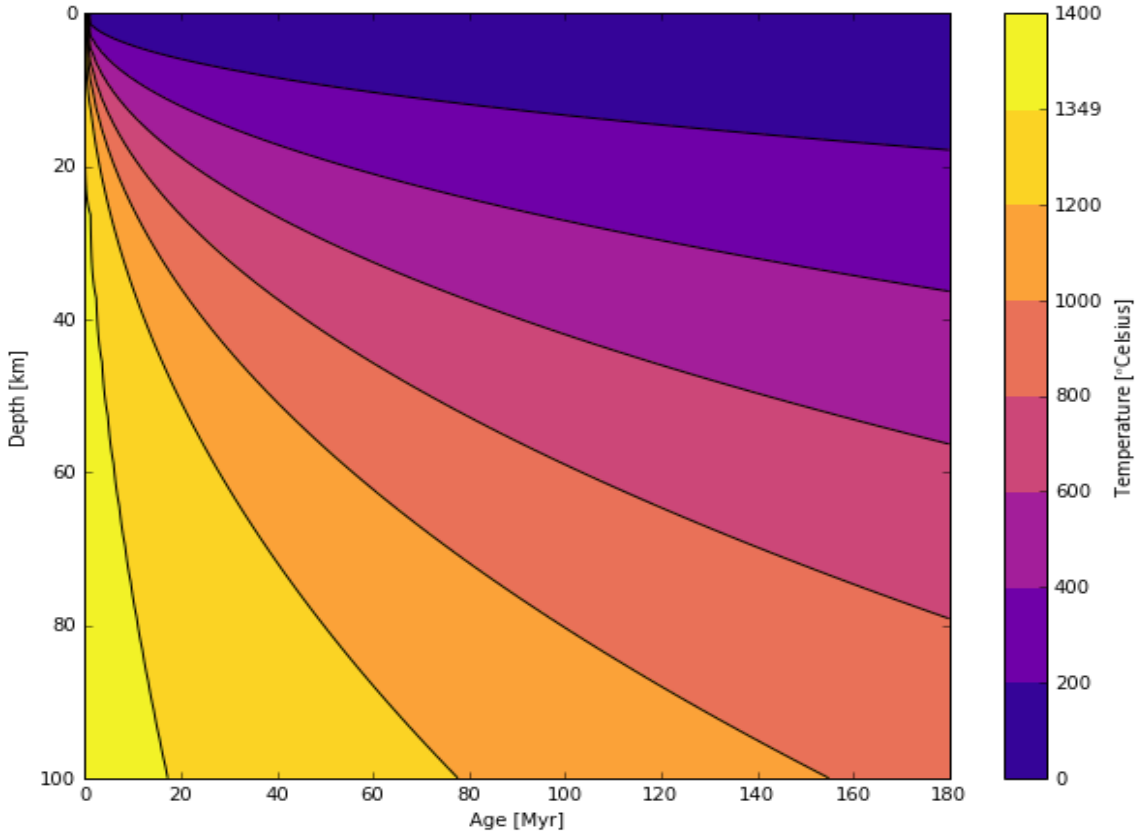

Figure 4: Calculated oceanic isotherms for half-space cooling model for age (0-180) Ma old lithosphere. The isotherms were computed from equation (2.1) using Tm = 1350OC, Ts = 0^0C and k = 1 x 10^{-6} m^2s^{-2}.

The half space cooling model (Turcotte and Oxburgh, 1967) only considers the non-adiabatic mantle. However, Faul and Jackson (2005) included an adiabatic component of the mantle to the model. The inclusion of the adiabatic component marks the boundary between the conductive lithosphere and the convective asthenosphere. Therefore, including the convective mantle to the conductive part the actual temperature increases due to the adiabatic gradient. The mathematical formula for the isotherm is thus;

$T(t, z) = Ts + (Tad - Ts)\ erf\ (1 + \frac{z}{2\sqrt{kt}})$... (2.2)

Where Tad is the adiabatic temperature gradient = $Tm\ (1+\alpha T\ [gz / C_p])$, where αT is the coefficient of thermal expansion, C_p is the specific heat at constant pressure, g is the acceleration due to gravity, and Ts is the temperature at sea floor and can be set to 0°C (Faul and Jackson, 2005).

2.1.2 Plate cooling model

The plate model has been defined as the most reliable model for calculating the temperature structure of ocean lithosphere (Mckenzie, 1967). Following the realization that ocean depth flatten at about 80 Ma (Parsons and Sclater, 1977; Davies and Lister, 1974; Renkin and Sclater, 1988), a plate model proposed by Mckenzie (1967) was adopted. In contrast to half space cooling model, the plate model is mathematically more cumbersome (Carlson et. al, 1994). However, the plate model is similar to half space cooling model for younger ages, but for older ages the effects of basal heating caused the depth and heat flow curves to flatten (fig. 5, top).

A simplified mathematical solution for temperature and heat flow was adopted from Stein and Stein (1992). The equation for the geotherm is written as:

$T(x,z) = T_m[z/a + \Sigma\ C_n \sin(n\pi z/a) \exp(-\beta_n\ x/a)]$... (2.3)

Where x, is the distance from the ridge crest, z, is the depth below the plate surface, a, is the thermal plate thickness, Tm is the basal temperature, and;

$C_n = 2/(n\pi)$, $\beta_n = (R^2 + n^2\pi^2)^{1/2} - R$, and $R = va/(2k)$

Where R is the Peclet number, which depends on the plate thickness a and velocity v.

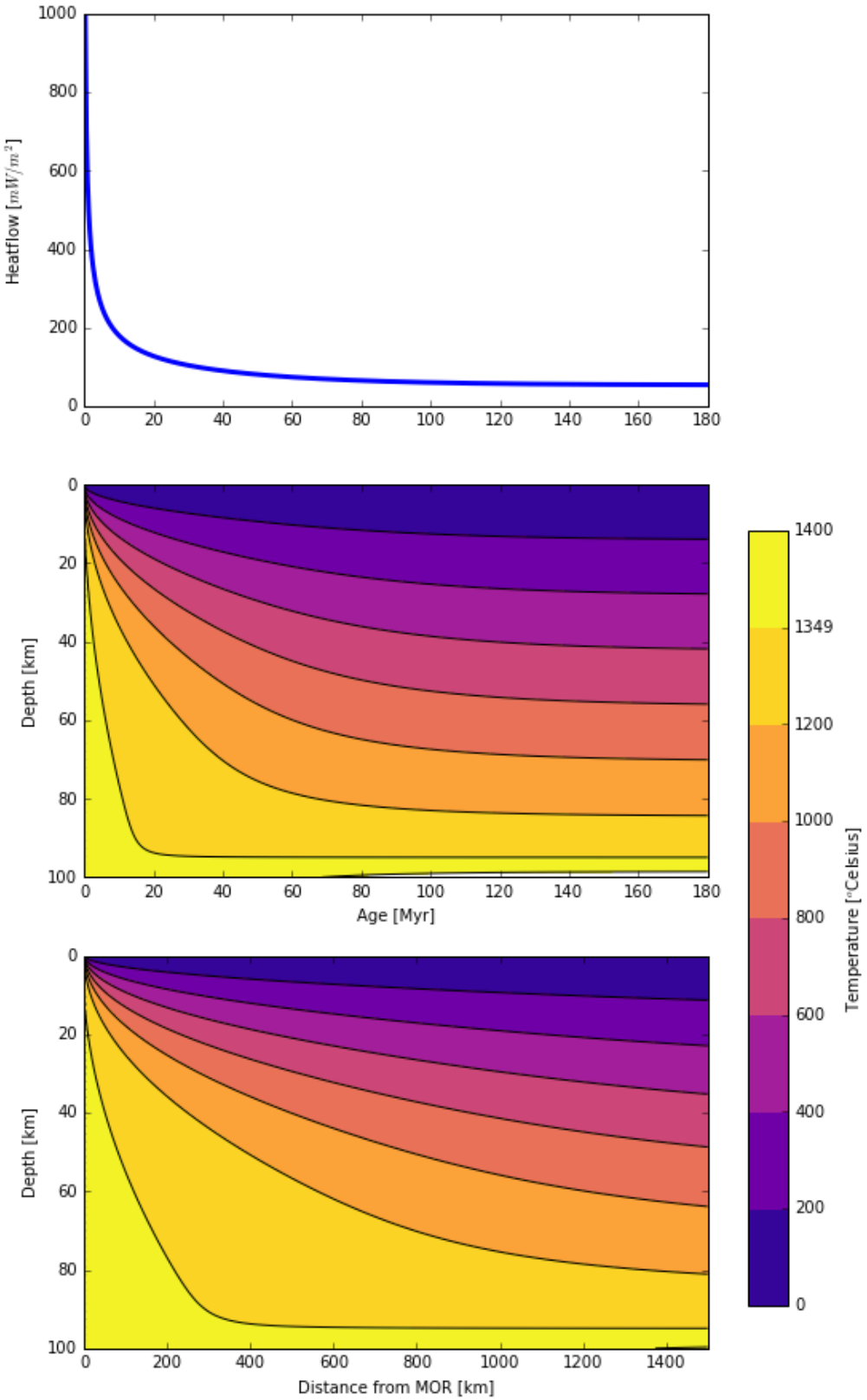

Figure 5: Plate model for thermal evolution of oceanic crust. (top) calculated heat flow Vs age plot, (middle) oceanic isotherms for age (0 – 180 Ma) old lithosphere and (bottom) relationship between depth of the ocean floor and distance from the mid-ocean ridge.

$R >> n\pi$ and $\beta_n x/a \sim (n^2 k\pi^2/a^2)t$, and t is the age of the plate. Equation (2.3) can be approximated to obtain:

$T(z,t) = T_m[z/a + \Sigma\, C_n \sin(n\pi z/a) \exp(-n^2 ct)]$… (2.4)

The heat flow as a function of age is given by:

$q(t) = q_m\,[1 + 2\,\Sigma \exp(-n^2 ct)]$… (2.5)

$q_m = K\,T_m / a$ and is the asymptotic heat flow for old seafloor.

Figure 5 (middle) shows oceanic isotherms for plate model with a higher basal temperature in comparison to half space cooling model. Asymptotic thickness of 95 Km and basal temperature of 1350°C with a spreading rate of 20mm/yr were used for the plot. The asymptotic thickness correlates with the depth above which temperature changes results in seafloor variations and below which extra heat is supplied.

Thus, old lithosphere maintains a constant thickness since the basal temperature is controlled by convection and younger lithosphere continue to cool. Several researchers have suggested a variety of reasons for the increased basal heating such as small-scale convection (Parsons and Mckenzie, 1978), radiogenic heat (Crough, 1977), shear heating (Schubert et al., 1976), and mantle plumes (Davies, 1988). Figure 5 (bottom) shows the variation of temperature with distance from the mid-ocean ridge. As observed from the profile the ocean depth increases away from the mid-oceanic ridge. Near the ridge axis the plates are hotter, thinner and hence slower seismic velocities. The farther away from the ocean ridges, the cooler the oceanic crust and the faster the seismic velocity. As a result of cooling, the oceanic crust becomes denser and subsides as it moves farther from the ridge crest.

3. Methodology

3.1 Data Collection

To ensure authenticity and reliability, data for this study were gathered from multiple sources and cross-referenced to remove inconsistencies. Heat flow measurements across various marine lithosphere regions were obtained from the International Heat Flow Commission database (2006). Seafloor age data, detailing the historical spread of oceanic lithosphere formation, were acquired from Müller et al. (2008). Geothermal gradient data were collected from previously published literature to calibrate theoretical models against observed thermal fluctuations. Seismic tomographic models were also used to validate theoretical predictions by comparing computed temperature distributions with velocity anomalies in seismic studies.

3.2 Analytical Method

The study employed both the half-space cooling model and the plate cooling model to predict temperature-depth relationships. Regression analysis was conducted to evaluate heat flow trends concerning crustal age. Theoretical thermal models were compared against observed seismic velocity anomalies to

determine model accuracy. A MATLAB-based numerical modeling approach was used to compute temperature distributions and visualize geotherm variations, ensuring a precise assessment of lithospheric thermal structure.

3.3 MATLAB Implementation

A MATLAB script was developed to implement the governing equations for both the half-space and plate cooling models. The script initialized parameters such as thermal diffusivity, mantle potential temperature, and lithospheric thickness. The compiled datasets were preprocessed into MATLAB-compatible structures for seamless integration into the computational framework. Using finite difference methods, the script solved the heat conduction equation to compute temperature profiles at varying depths and lithospheric ages. Temperature-depth profiles were generated to visualize cooling trends and compare them with observed seismic data. Heat flow values were calculated and compared against empirical data to assess the accuracy of each cooling model. Statistical analyses were performed on numerical outputs to quantify model reliability and ensure consistency with observed thermal structures.

4. Results and Discussion

4.1. Predicted temperatures (1-D)

Analysis of different plots (for both older and younger age lithosphere) of geotherms for the half space cooling model can be used to estimate the temperatures within sediments as well as the estimation of lithospheric thickness. Similarly, older age geotherms have lower mantle temperatures, but have deeper roots, whereas, younger age geotherms have higher mantle temperatures at shallow levels. For example, 40Ma geotherm have a maximum thickness of about 79 Km, whereas, 120Ma geotherm have a maximum depth of about 119 km (fig. 6).

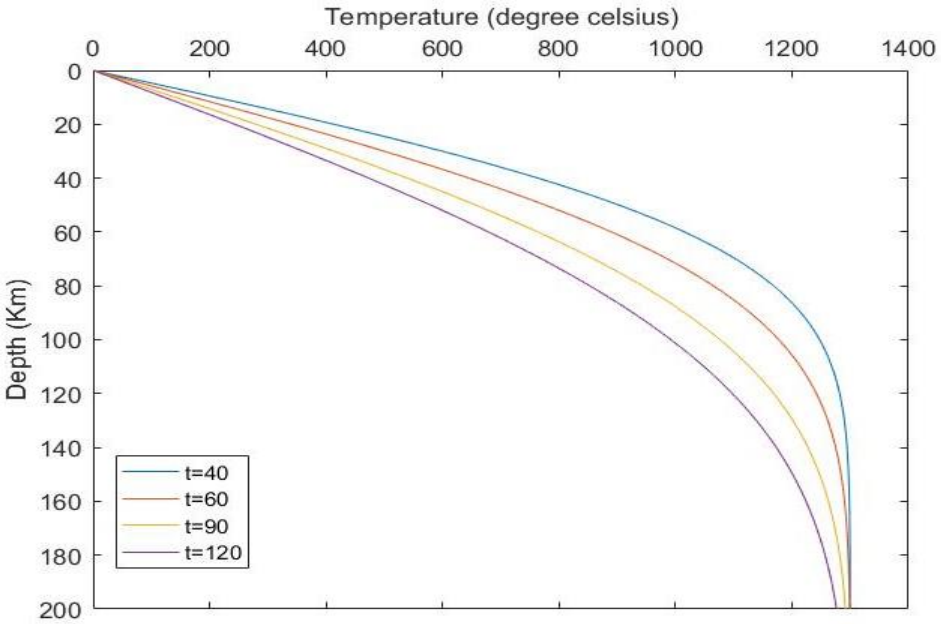

Figure 6: Conductive geotherms for oceanic lithosphere for 40, 60, 90 and 120 Ma.

4.2 . Difference in temperature versus depth plots

Plotting the difference in temperature between varying age lithosphere shows a number of features that can be expected for the half space cooling model:

Large differences in temperature for older ages were observed. For instance, when comparing 40 and 60Ma (fig. 7) oceanic lithosphere the maximum temperature difference is at 54km depth. In contrast, comparing 40 and 120Ma oceanic lithosphere gives a maximum temperature difference at 61km depth. If we assume a linear relationship between temperature and velocity, one would expect a greater velocity difference for older 80Ma lithosphere (120-40Ma) compared to the younger 20Ma lithosphere (60-40Ma).

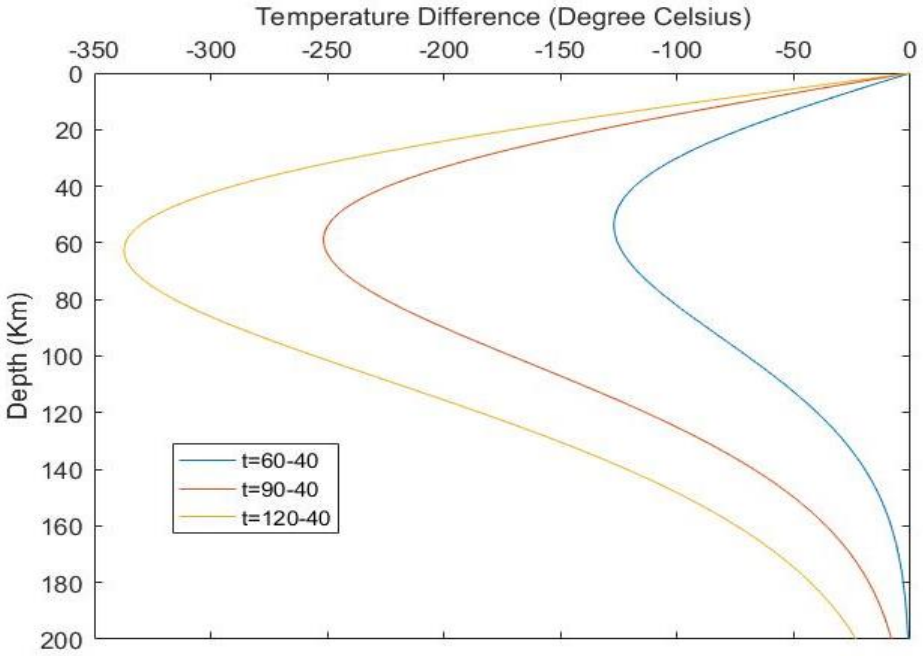

Figure 7: Temperature difference with depth plots for ages; 60-40, 90-40 and 120-40 Ma.

Similarly, temperature difference versus depth plots for 80Ma difference between younger and older geotherms (fig. 8) shows a higher maximum temperature difference for younger geotherms (90-10Ma), intermediate maximum temperature difference for 120-40Ma geotherms and a lower maximum temperature difference for the older geotherm (200-120Ma). The younger (90-10Ma) geotherm will have a greater difference in velocity compared to 120-40Ma geotherm. The older geotherm will have the least velocity difference. Point of intersection between 90-10 and 120-40Ma geotherms gives a temperature difference of -300.2°C at 86Km depth. Geotherms (90-10 and 200-120Ma) converge at a temperature difference of about -154.9°C and 113Km depth. Also, 120-40 and 200-120Ma geotherms intersects at a temperature difference of -139.5°C and 133Km depth.

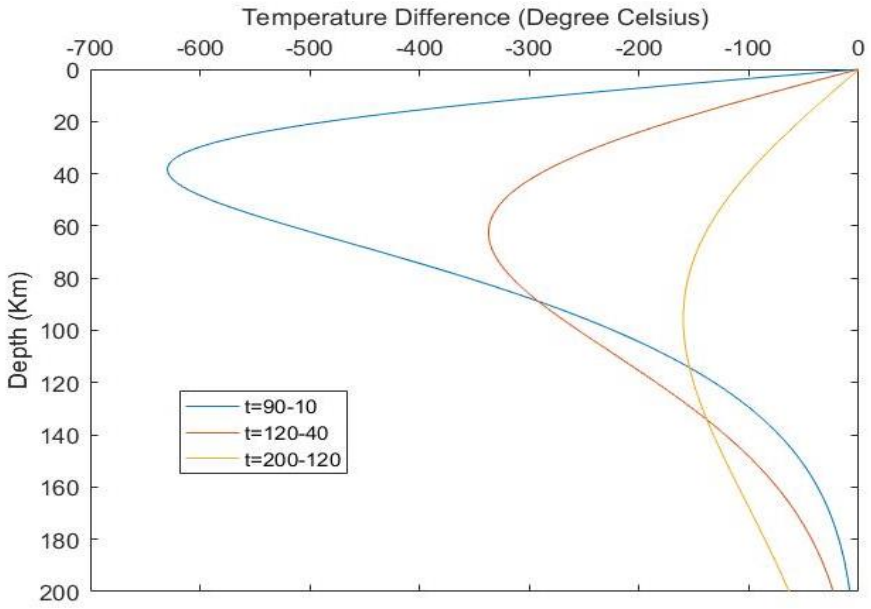

Figure 8: Temperature difference with depth plots for 90-10, 120-40 and 200-120 Ma.

4.3. Variation due to changing mantle potential temperature (Tm)

Oceanic geotherms (fig. 9) with varying mantle potential temperatures between 1200 – 1400°C shows an increasing mantle temperature difference with depth. Comparatively geotherms between 1200 and 1400°C gives temperature difference of about 25°C at 20 km depth. Looking deeper levels, at 40, 80, 100, 140 and 200km depths gives corresponding temperature differences of 98°C, 144°C, 154°C, 191°C and 198°C. Variation in mantle potential temperatures alters the temperature-depths profiles. For example, in areas affected by a mantle plume or upwelling, mantle potential temperature may be expected to be higher.

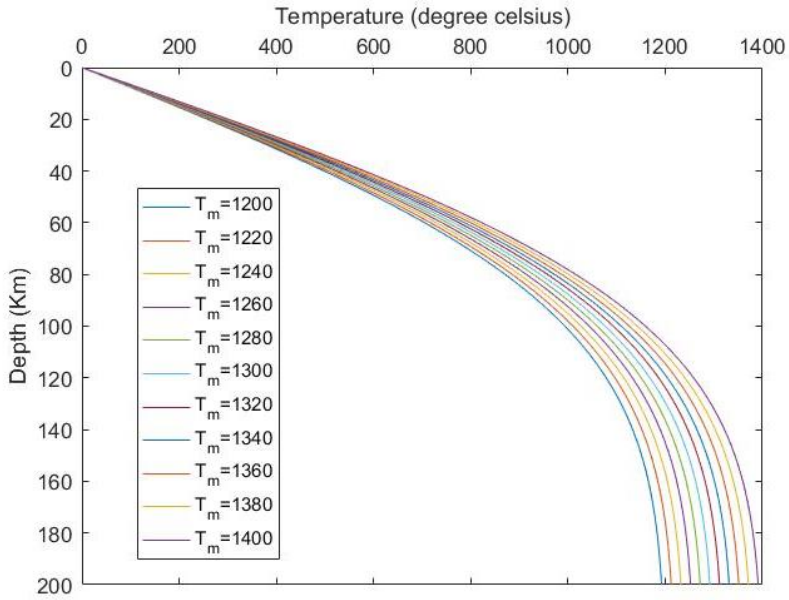

Figure 9: Plot of mantle geotherms for oceanic lithosphere varying mantle potential temperatures (Tm) between 1200 and1400°C.

4.4. Predictions for the West African Margin

The predicted temperature structure for the Western margin of Africa has been computed using both the half-space and plate cooling models (with asymptotic thickness of 95km and 130km). In both models (above 100km) an adiabatic gradient was assumed to account for the convective mantle. The subsurface temperature from both models is maximum at ocean ridges and decreases towards the continent (fig. 10, 11 and 12). In addition, at 50km depth, the two models show colder lithosphere away from the ridge. These low temperature regions are interpreted as areas of fast seismic velocities, thicker, and older. Beneath the ridge axis there is a narrow region of high temperature which is due to upwelling of hot materials from the mantle. These high temperature regions beneath the ocean ridges are areas of slow seismic velocity anomalies, hotter, and younger.

Similar plot for half-space cooling model at 100km depth (fig. 13) reveal a broad high temperature beneath the ridge axis. These high temperature beneath the ridge are interpreted as areas of slow seismic velocities and younger. The low temperature feature observed away from ocean ridges at 100km depth for half-space cooling model is due to the fact that the model assumes a continuous cooling for all ages. The temperature map for plate model (fig. 14) with asymptotic thickness of 95 km at 100 km depth shows a uniform temperature gradient beneath both the ocean ridge and away from the ridge. However, the homogenous feature is due to the fact that the geothermal gradient is no longer controlled by conductive cooling, but by adiabatic compression. The geothermal gradient for adiabatic compression is much smaller compared to gradient in the conductive lithosphere. On the contrary, the plate model (fig. 15) with asymptotic thickness of 130km and mantle potential temperature of 1330°C, shows a colder lithosphere away from the ridge. This is because at 100km depth it is still below the asymptotic thickness (a = 130km) and it is still controlled by conductive cooling.

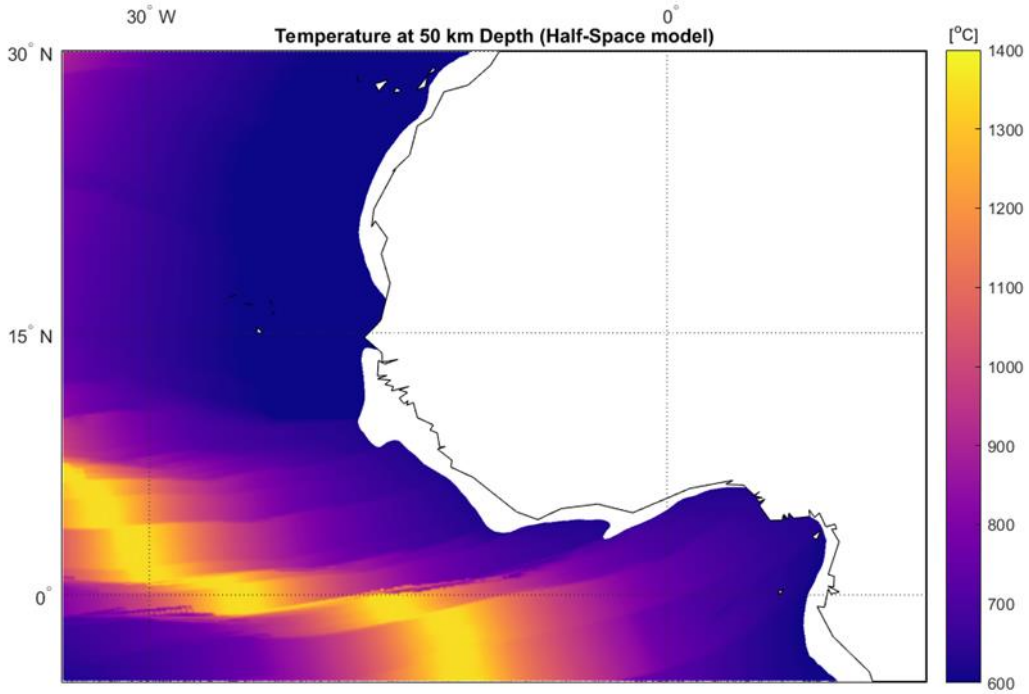

Figure 5: Temperature map at 50km depth with mantle potential temperature (Tm=1350°C) for the western coast of Africa using half-space cooling model.

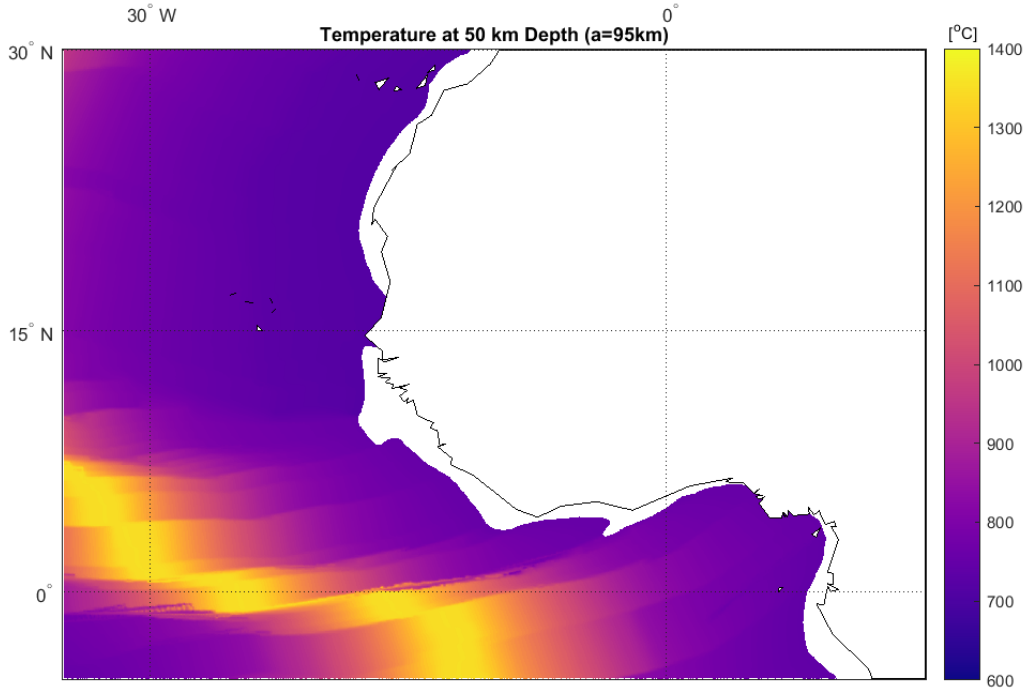

Figure 6: Temperature map at 50km depth for plate model with asymptotic thickness of 95 km and mantle potential temperature of 1350°C.

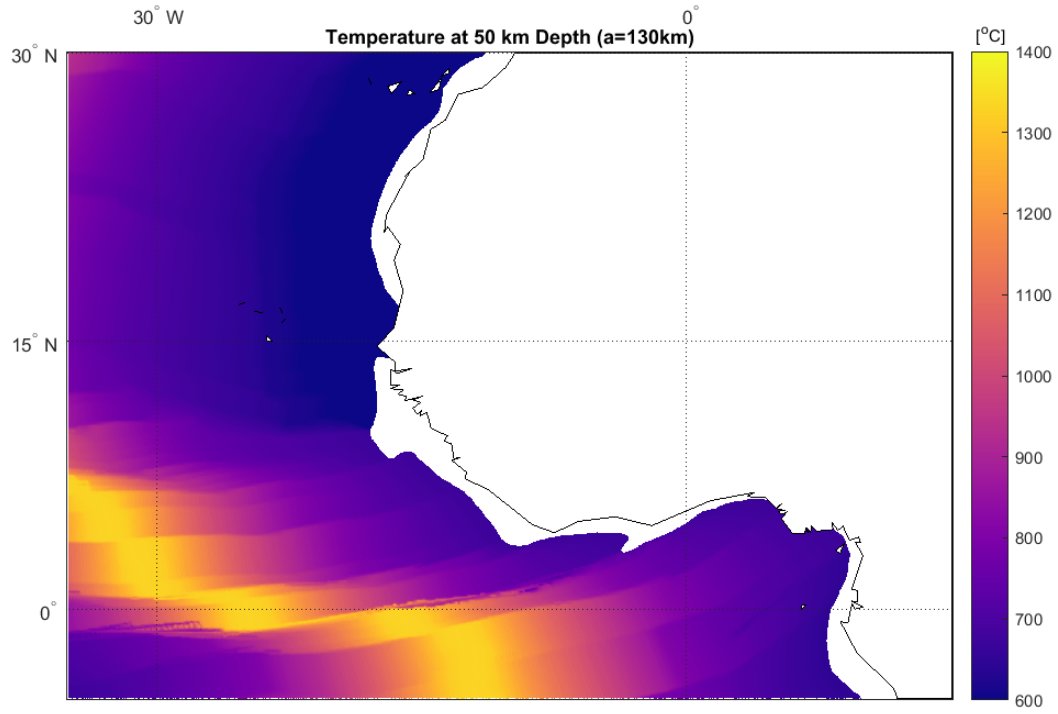

Figure 7: Temperature map at 50km depth for plate model with asymptotic thickness of 130 km and mantle potential temperature of 1330°C.

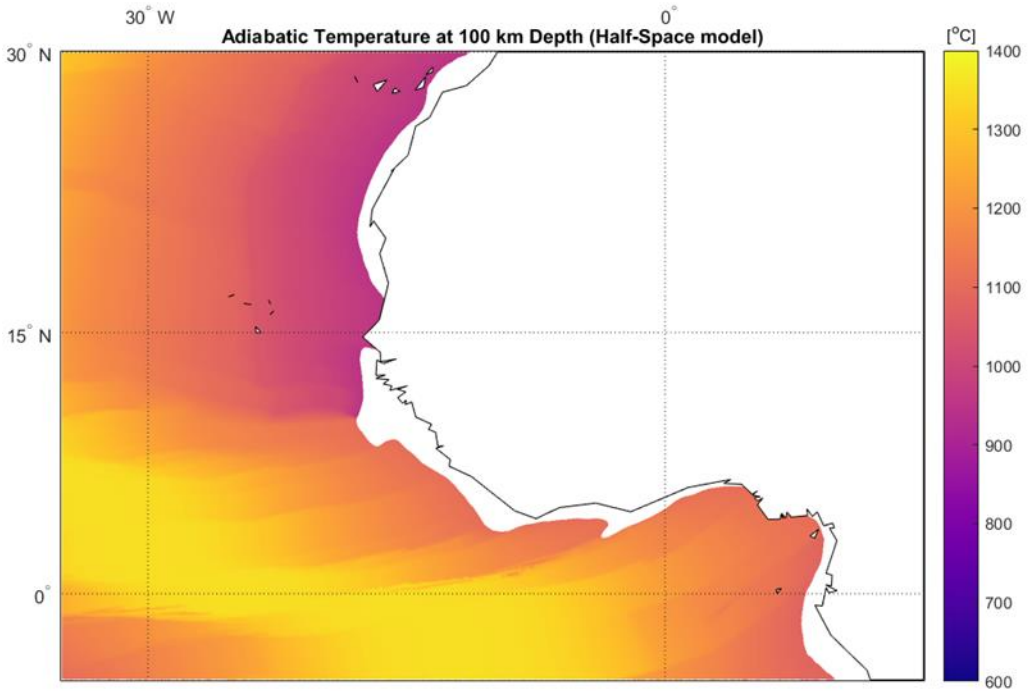

Figure 8: Temperature map at 100km depth with adiabatic component and mantle potential temperature (Tm=1350°C) for the western coast of Africa using half-space cooling model.

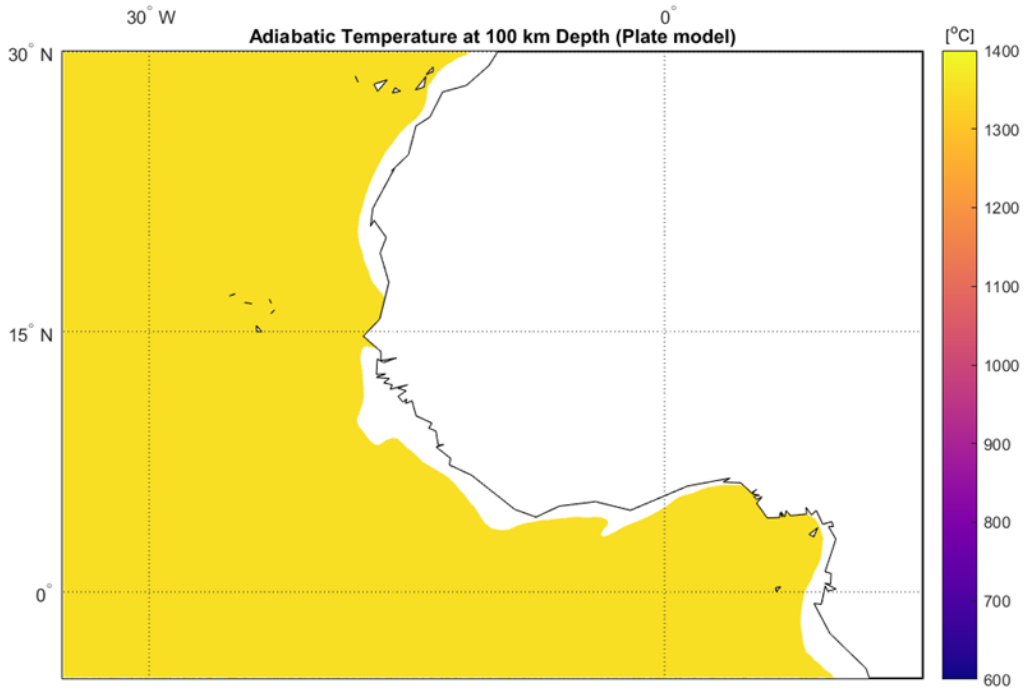

Figure 9: Temperature map at 100km depth for plate model with adiabatic gradient of 0.4°C/Km and an asymptotic thickness of 95 km and mantle potential temperature of 1350°C.

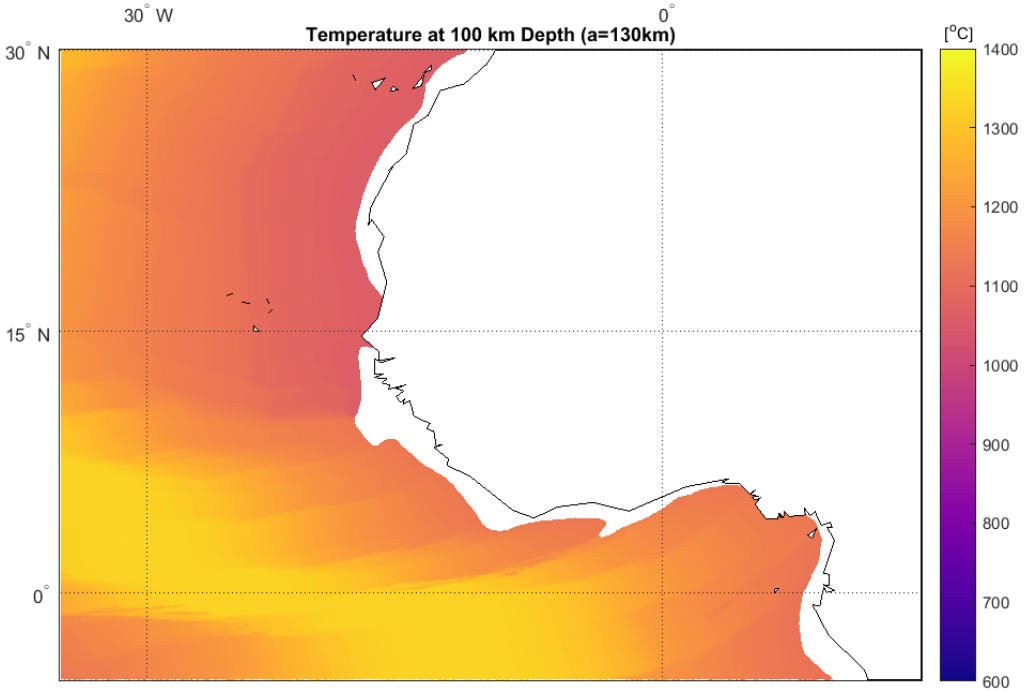

Figure 10: Temperature map at 100km depth for plate model with adiabatic gradient of 0.4°C/Km and an asymptotic thickness of 130km and mantle potential temperature of 1330°C.

4. Conclusion

This study reinforces the applicability of thermal models in assessing lithospheric evolution. Comparison of the cooling models shows that at 50 km depth, both models show cooler lithosphere away from the ridge, with high temperatures at the ridge axis corresponding to slow seismic velocities. However, at 100 km depth, the half-space model predicts a broad high-temperature anomaly, while the plate model shows a uniform temperature gradient due to adiabatic compression. The plate model provides a better fit for older oceanic lithosphere, while the half-space model is suitable for younger regions. Future research should integrate refined seismic velocity models to enhance understanding of the thermal and mechanical evolution of the lithosphere along the Western Coast of Africa.

References

Brown, C., 1994. Tectonic interpretation of regional conductivity anomalies. *Surveys in Geophysics*, *15*(2), pp.123-157.

Bullard, E.C., 1952. Heat flow through the floor of the eastern North Pacific Ocean. *Nature*, *170*(4318), pp.200-200.

Bullard, E.C., 1945. Thermal history of the Earth. *Nature*, *156*(3950), pp.35-36.

Bullard, E.C., 1939. Heat flow in South Africa. *Proceedings of the Royal Society of London. Series A, Mathematical and Physical Sciences*, pp.474-502.

Carlson, R.L. and Johnson, H.P., 1994. On modeling the thermal evolution of the oceanic upper mantle: An assessment of the cooling plate model. *Journal of Geophysical Research: Solid Earth*, *99*(B2), pp.3201-3214.

Crosby, A.G., 2006. *Aspects of the relationship between topography and*

gravity on the Earth and Moon (Doctoral dissertation, University of Cambridge).

Crough, S.T., 1977. Isostatic rebound and power-law flow in the asthenosphere. *Geophysical Journal International*, *50*(3), pp.723-738.

Davies, J.H. and Davies, D.R., 2010. Earth's surface heat flux. *Solid Earth*, *1*(1), p.5.

Davies, G.F., 1988. Ocean bathymetry and mantle convection: 1. large-scale flow and hotspots. *Journal of Geophysical Research: Solid Earth*, *93*(B9), pp.10467-10480.

Davis, E.E. and Lister, C.R.B., 1974. Fundamentals of ridge crest topography. *Earth and Planetary Science Letters*, *21*(4), pp.405-413.

Faul, U.H. and Jackson, I., 2005. The seismological signature of temperature and grain size variations in the upper mantle. *Earth and Planetary Science Letters*, *234*(1), pp.119-134.

Fishwick, S., 2010. Surface wave tomography: imaging of the lithosphere–asthenosphere boundary beneath central and southern Africa?. *Lithos*, *120*(1), pp.63-73.

Forte, A.M., Woodward, R.L. and Dziewonski, A.M., 1994. Joint inversions of seismic and geodynamic data for models of three—dimensional mantle heterogeneity. *Journal of Geophysical Research: Solid Earth*, *99*(B11), pp.21857-21877.

Goutorbe, B., 2010. Combining seismically derived temperature with heat flow and bathymetry to constrain the thermal structure of oceanic lithosphere. *Earth and Planetary Science Letters*, *295*(3), pp.390-400.

Hasterok, D., 2013. A heat flow based cooling model for tectonic plates. *Earth and Planetary Science Letters*, *361*, pp.34-43.

Hillier, J.K. and Watts, A.B., 2005. Relationship between depth and age in the North Pacific Ocean. *Journal of Geophysical Research: Solid Earth*, *110*(B2).

Hoggard, M.J., Winterbourne, J., Czarnota, K. and White, N., 2017. Oceanic residual depth measurements, the plate cooling model, and global dynamic topography. *Journal of Geophysical Research: Solid Earth*, *122*(3), pp.2328-2372.

Jaupart, C., Labrosse, S. and Mareschal, J.C., 2007. 7.06--Temperatures, heat and energy in the mantle of the earth. *Treatise on geophysics*, *7*, pp.223-270.

Johnson, H.P. and Carlson, R.L., 1992. Variation of sea floor depth with age: a test of models based on drilling results. *Geophysical Research Letters*, *19*(19), pp.1971-1974.

Langseth, M.G., Le Pichon, X. and Ewing, M., 1966. Crustal structure of the mid-ocean ridges: 5. Heat flow through the Atlantic Ocean floor and convection currents. *Journal of Geophysical Research*, *71*(22), pp.5321-5355.

Lee, W.H. and Uyeda, S., 1965. *Review of heat flow data* (pp. 87-190). American Geophysical Union.

Müller, R.D., Sdrolias, M., Gaina, C. and Roest, W.R., 2008. Age, spreading rates, and spreading asymmetry of the world's ocean crust. *Geochemistry, Geophysics, Geosystems*, *9*(4).

McKenzie, D., Jackson, J. and Priestley, K., 2005. Thermal structure of oceanic

and continental lithosphere. *Earth and Planetary Science Letters*, *233*(3), pp.337-349.

McKenzie, D.P. and Sclater, J.G., 1969. Heat flow in the eastern Pacific and sea floor spreading. *Bulletin Volcanologique*, *33*(1), pp.101-117.

McKenzie, D.P., 1967. Some remarks on heat flow and gravity anomalies. *Journal of Geophysical Research*, *72*(24), pp.6261-6273.

Parsons, B. and McKenzie, D., 1978. Mantle convection and the thermal structure of the plates. *J. geophys. Res*, *83*(B9), pp.4485-4496.

Parsons, B. and Sclater, J.G., 1977. An analysis of the variation of ocean floor bathymetry and heat flow with age. *Journal of geophysical research*, *82*(5), pp.803-827.

Pollack, H.N., Hurter, S.J. and Johnson, J.R., 1993. Heat flow from the Earth's interior: analysis of the global data set. *Reviews of Geophysics*, *31*(3), pp.267-280.

Pollack, H.N. and Chapman, D.S., 1977. On the regional variation of heat flow, geotherms, and lithospheric thickness. *Tectonophysics*, *38*(3-4), pp.279-296.

Ritzwoller, M.H., Shapiro, N.M. and Zhong, S.J., 2004. Cooling history of the Pacific lithosphere. *Earth and Planetary Science Letters*, *226*(1), pp.69-84.

Renkin, M.L. and Sclater, J.G., 1988. Depth and age in the North Pacific. *Journal of Geophysical Research: Solid Earth*, *93*(B4), pp.2919-2935.

Schubert, G., Froidevaux, C. and Yuen, D.A., 1976. Oceanic lithosphere and asthenosphere: thermal and mechanical structure. *Journal of Geophysical Research*, *81*(20), pp.3525-3540.

Sleep, N.H., 2005. Evolution of the continental lithosphere. *Annu. Rev. Earth Planet. Sci.*, *33*, pp.369-393.

Stein, S. and Wysession, M., 2003. An introduction to seismology, earthquakes, and earth structure.

Stein, C. A., and Stein, S., 1992. A model for the global variation in oceanic depth and heat flow with lithospheric age. *Nature*, *359*(1).

Turcotte, D.L. and Schubert, G., 2002. Geodynamics, Cambridge University Press. *New York*, pp.164-165.

Turcotte, D.L. and Oxburgh, E.R., 1967. Finite amplitude convective cells and continental drift. *Journal of Fluid Mechanics*, *28*(01), pp.29-42.